EasyChair Preprint

№ 15294

Preliminary Wind Resource Assessment at the Mearim River Edge

Juan Ibanez, Rafael Veras, Henzo Costa, Arcilan Assireu, Denivaldo Lopes, Denisson Oliveira, Osvaldo Saavedra and Shigeaki Lima

October 24, 2024

Preliminary Wind Resource Assessment at the Mearim River Edge

Juan D. F. Ibanez * **Rafael B. de S. Veras** * **Henzo C. de Jesus** *
Arcilan T. Assireu ** **Denivaldo Lopes** * **Denisson Q. Oliveira** *
Osvaldo R. Saavedra * **Shigeaki L. de Lima** *

* *Instituto de Energia Elétrica, Universidade Federal do Maranhão, MA, (juan.ibanez, rafael.brito, henzo.costa)@discente.ufma.br, denivaldo.lopes@ufma.br, dq.oliveira@ufma.br, osvaldo.saavedra@ufma.br, shigeaki.lima@ufma.br*
** *Instituto de Ciências Naturais, Universidade Federal de Itajubá, MG, arcilan@unifei.edu.br*

Abstract: This study presents a significant initial assessment of the wind potential of the Bacabeira region in the Brazilian state of Maranhão, using data from a Sonic Detection and Ranging (SODAR) station installed on the eastern bank of the Mearim River. Our preliminary findings suggest substantial wind potential, highlighting favorable geographic characteristics that support wind energy exploitation. For the evaluation of the region's energy potential, a measurement period was stablished using a SODAR, with wind data measured by profiling. Two methodologies were then applied for estimating turbine power output: the rotor equivalent wind speed (REWS) and the hub height method. The region proved promising for this kind of energy exploitation, presenting daily capacity factors up to 0.70 in a month of moderate winds in the area.

Keywords: Renewable energy; Wind potential; SODAR profiling; Northwest Brazil; REWS.

1. INTRODUCTION

Wind energy in Northeast Brazil represents a significant and growing segment of Brazil's renewable energy portfolio. This region, known for its steady and strong winds, is particularly suitable for wind energy production as seen in (ABEEÓLICA, 2022). The development of wind energy in Northern Brazil is part of Brazil's broader efforts to increase renewable energy sources and reduce its dependence on traditional fossil fuels.

The unique geographical and climatic conditions of Northeast Brazil, including its extensive coastline and the presence of consistent trade winds, provide an ideal environment for wind farms (Dantas et al., 2019). These features contribute to high-capacity factors, meaning that wind turbines in this region can produce electricity close to their maximum potential more frequently than in many other parts of the world (ONS, 2023).

Wind energy in Northern Brazil is a dynamic and vital part of Brazil's push towards a more sustainable and environmentally friendly energy future. With continued investment and careful management, it promises to provide a substantial portion of Brazil's electricity needs while also contributing to global efforts to mitigate climate change.

The coastline of the region has demonstrated significant potential for wind energy generation, turning it apt to the establishment of several efficient wind farms. As available coastal areas approach full capacity, it becomes strategically important to explore adjacent regions that retain similar coastal energy characteristics. Conducting technical and economic feasibility studies will be crucial in determining whether these areas are suitable for current or future wind farm development.

In this paper, we present preliminary studies on wind energy conducted in the Mearim River region, located 30 km from the entrance to São Marcos Bay in Maranhão. According to (Costa et al., 2023), this coastal area, characterized by its partial flooding, low vegetation, and minimal conflict with other land uses, provides a unique setting for such research. Over several months, data were collected using a Sonic Detection and Ranging (SODAR) platform, and additionally, point-specific data were gathered using an onboard Light Detection and Ranging (LIDAR) system better addressed by (Figueredo et al., 2023).

This paper is structured as follows: Section 2 provides a description of the location, Section 3 discusses the data analysis conducted during the measurements, Section 4 addresses the generation modeling, Section 5 presents the results and Section 6 concludes the paper.

2. SITE DESCRIPTION

The wind resource monitoring system was installed on a shrimp farm located near the Mearim River / São Marcos Bay, 30 km from São Luís, in the village of Perises de Baixo, municipality of Bacabeira/MA, BR-315. This region is characterized by an extensive fluvio-marine plain as described above (Cosme et al., 2023), with halophytic floodplain fields. Access to the farm is via a local road,

partly paved with asphalt and partly dirt. Fig. (1a) and Fig. (1b) show the satellite images of this location.

Also in Fig. (1a), it is possible to observe the proximity of the measurement site to the Mearim River (approximately 2 km) and Caranguejo Island (a site of previous studies conducted by our research team). The location represented by the white dotted circle indicates the tanks for shrimp farming in captivity. Due to the proximity to the Mearim River, it is possible to assert that the wind resource measured at this point Fig. (1b) also represents approximately the same wind conditions within a radius of 5 km, since it is a field that remains flooded for much of the year with lowlying vegetation and, when present, lowheight mangrove vegetation.

(a) Prospecting area near the Mearim River. (b) Exact area of wind prospecting.

Figure 1. Maps showing the prospecting areas.

The reason for developing studies in this area stems from several favorable aspects it presents. The proximity to the capital, São Luís, and particularly to the electrical transmission network (230 kV substations), along with the low land costs (lands poor for cultivation) and easy access (logistics facilitated by road and rail networks, close to ports), could be attractive for the installation of wind farms. Thus, the commercial wind resource between 40 m and 160 m in altitude is the focus of the discussion in this paper.

The wind resource measurement campaigns were conducted using a Sonic Detection and Ranging (SODAR) wind profiler, seen in Fig. (2), which shows the location of its installation between two shrimp breeding tanks in a flat and open area.

Figure 2. SODAR installed at the measurement point.

Since it is a remote location, the electrical service is supplied by a rural energy provider, primarily used for pumping in the water renewal of the tanks.

Given the irregularity in the power supply and the delays in restoration, it was necessary to use an uninterruptible power supply (UPS) with a remote access control panel, as shown in the figure below Fig. (3), to ensure a reliable energy supply to the SODAR and its accessories.

Figure 3. SODAR nanogrid setup at the measurement site.

The support system consists of an uninterruptible power supply (UPS) that feeds in parallel with the existing electrical network, the SODAR converter (220 V AC / 24 V DC), and an internal power supply (220 V AC / 24 V DC) located in the control panel. This device allows energy supply to an industrial computer (which runs the SODAR software collecting measurement data) and a 4G

modem that enables remote access to the database, as well as monitors the proper operation of the system.

This system allowed for the reliable storage of data on a server and facilitated remote access for maintenance, ensuring continuous and efficient operation.

3. DATA ANALYSIS

The measurements were conducted from December 1st to 27th, 2023, a period marked by heavy rainfall in the Perizes region. The SODAR was configured to measure heights ranging from 30 m to 280 m, with a frequency of 10 minutes. In total, 99,866 valid entries were obtained. The wind speed is illustrated at heights of 40 m, 100 m, and 160 m, as detailed in Figure 4.

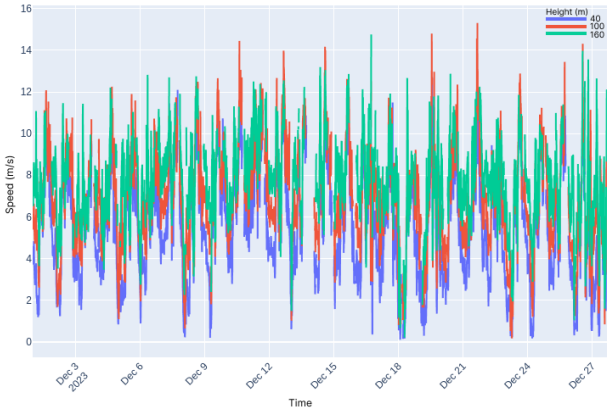

Figure 4. Wind Speed Measurements for Heights of 40 m, 100 m and 160 m for the Month of December.

A small gap in the data was observed at certain heights. This is due to a temporary shutdown of the equipment caused by the lack of a reliable power grid and some necessary maintenance. At 40 m height, wind speed peak reaches approximately 12 m/s. At 100 m, the peak reaches 14 m/s, and for 160 m, it reaches around 15 m/s. In Fig. (5), daily measurements of the average wind speed at heights of 40 m, 100 m and 160 m are presented.

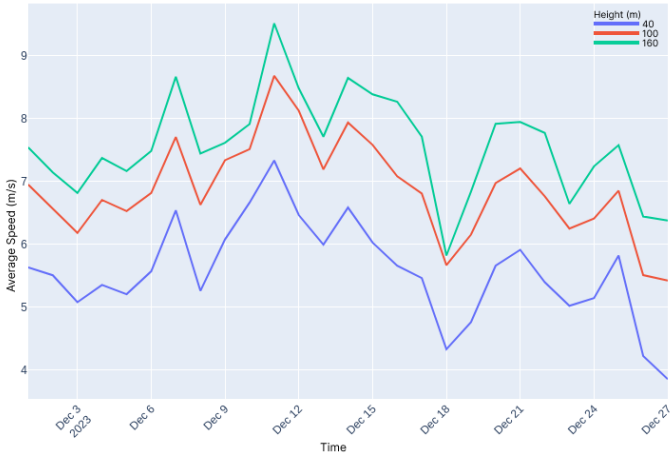

Figure 5. Daily Average Wind Speed Measurements for Heights of 40 m, 100 m and 160 m for the Month of December.

In Fig. (5), we observe the variation in average wind speed at heights of 40 m, 100 m, and 160 m. The chart clearly illustrates how wind speed changes with height, highlighting peaks at different levels and variations over the measured period. There is a noticeable decrease in wind speed measurements on the 18th, likely due to rain. Even at 40 m height, there is a peak slightly above 7 m/s; at 100 m, a peak above 8 m/s; and at 160 m, a peak above 9 m/s. Additionally, at 40 m, the speed is still notable, considering that the normal cut-in speed of turbines is 3 m/s and, for most of the time, the speed at 40 m remains above 4 m/s. Between 100 m and 160 m, the average speed is similar and mostly above 6 m/s, while at 40 m, the speed is significantly lower.

We performed a statistical analysis using the database for heights of 40 m, 100 m and 160 m, and the results can be seen in Table 1.

Table 1. Statistical Comparison of Measured Speeds at Heights of 40 m, 100 m and 160 m.

Height(m)	40	100	160
Average (m/s)	5.58	6.86	7.56
Median (m/s)	5.49	6.71	7.62
StD (m/s)	2.52	2.35	1.99
Variance $(m/s)^2$	6.34	5.51	3.96
Minimum (m/s)	0.10	0.16	0.20
Maximum (m/s)	12.90	15.31	14.76
Amplitude (m/s)	12.80	15.15	14.56
1º Quatile (m/s)	3.65	5.36	6.39
3º Quartile (m/s)	7.42	8.40	8.76
IQR (m/s)	3.77	3.04	2.37
Availability	0.94	0.91	0.73

Based on the values presented in Table 1, referring to the data collected at Perizes, it is observed that the higher the altitude, the greater the wind speed. Specifically, the average wind speeds are 5.58 m/s at height of 40 m, 6.86 m/s at height of 100 m, and 7.56 m/s at height of 160 m. It is worth noting that variance decreases and data availability decreases as altitude increases.

With the data, we can construct a wind rose based on wind speed and direction. Furthermore, it is possible to compare the wind direction at heights of 40 m and 160 m. It is worth remembering that the higher the altitude, the smaller the variation in wind direction, as we will see below.

At height of 160 m, we have 3841 entries, of which 2810 do not have null data, corresponding to 73.16% valid data. We can analyze the wind behavior for this height through the wind rose in Fig. (6).

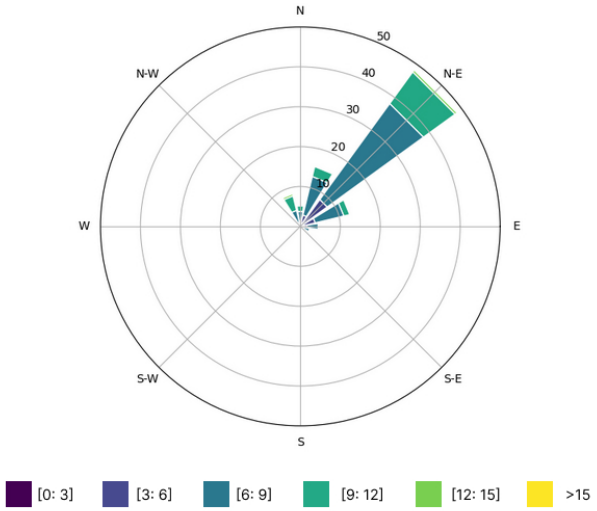

Figure 6. Wind Rose for 160 m Height in December.

Most occurrences were between the wind speeds of 6 m/s and 9 m/s, representing approximately 50% of the cases, as shown in Fig. (6). This speed range is suitable for turbines. Additionally, there were very few occurrences below the wind speed of 3 m/s. We also noticed that the wind direction is predominantly northeast (NE). For the height of 40 m, we recorded 3841 entries, of which 3639 do not have null data, corresponding to 94.74% valid data. Through the wind rose presented in Fig.(7)

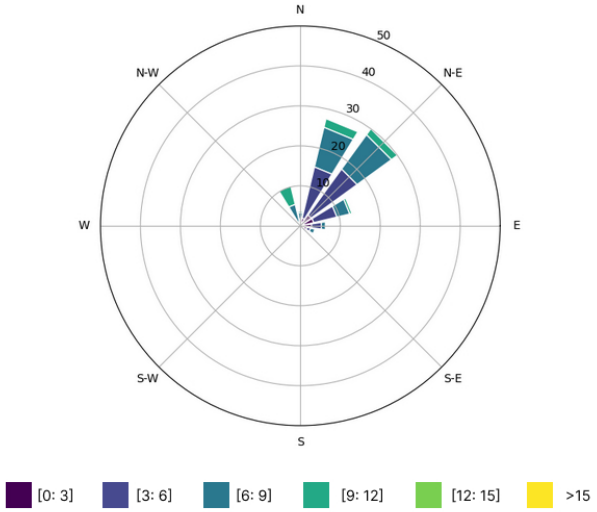

Figure 7. Wind Rose for 40 m Height in December.

Using a wind rose for a height of 40 m, we can observe a greater variation in wind direction towards the northeast-northeast and a significant decrease in wind speed compared to Figure (6). This indicates a strong influence of terrain roughness at this altitude.

4. ENERGY MODELING

Based on the wind data, it is now possible to estimate the installation of a potential wind turbine on site. The most common approach to estimate the power output of a specific turbine model is by using its power curve (P(W speed)) provided by the manufacturer, along with the velocity vector at the same height as the selected turbine's hub. In this study, we have chosen the Siemens 2.3-113 for energy generation analysis. This choice was made because its technical characteristics closely match those of the GE Energy 2.3-116, which is used in the nearest wind farm, Delta 6, in the region and its power curve, Figure 8, was made available by the manufacturer. Both turbines have a cut-in speed of 3 m/s, a rated power of 2.3 MW, and a rated wind speed close to 10.5 m/s (The-Wind-Power, 2018).

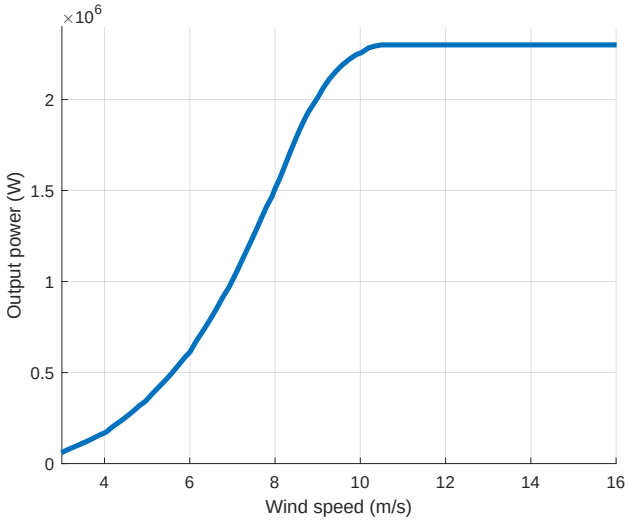

Figure 8. Siemens 2.3-113 wind turbine power curve.

Due to higher surface roughness, onshore wind behavior typically exhibits more pronounced wind shear, with intensity decreasing closer to the ground (Panofsky and Townsend, 1964). This phenomenon was pronounced in the study area, as shown in Fig. (5) and Table 1. The difference in average wind speed measured at heights of 40 m and 160 m is approximately 2 m/s. The wind speed at 40 m height shows a variance of 6.34 compared to 3.96 at 160 m height. These numbers indicate that not only does the wind intensity decrease at heights closer to the surface, but also its consistency declines. This phenomenon of wind variation with height is known as wind shear.

A high wind shear results in different wind intensities reaching the turbine rotor across its area. Consequently, relying solely on wind intensity data at the turbine hub height might lead to inaccuracies in estimating energy generation, as the actual wind intensity perceived by the turbine integrates intensities at different heights across the swept area of the turbine blades (Martins et al., 2023).

To address this issue, in addition to calculating power using the wind speed at the turbine hub height, the methodology proposed by (Sumner and Masson, 2006) will also be applied. This involves integrating the wind speed along the z-axis over the entire area swept by the turbine blades, as described by equation 1. The term 'Ueq' refers to the equivalent wind speed, which is calculated considering atmospheric stability. This measure represents the wind speed over the entire rotor disk area, rather than just at the specific height of the hub.

$$U_{eq} = \frac{2}{A_t} \int_{H-r}^{H+r} U(z) \left(r^2 - H^2 + 2Hz - z^2\right)^{1/2} \, dz \quad (1)$$

where $U(z)$ is the wind speed in (m s^{-1}) at the height z, and H, r, and A are, respectively, the hub height, the radius and the rotor area of the wind generator.

Since this measurement was conducted using a profiler, wind measurements for the entire area swept by the turbine blades under study are available every 10 m in height. The wind turbine equivalent will be integrated from 40 m to 160 m. Table 2 statistically compares the equivalent wind speed intensity calculated from Equation 1 with the measured intensities at 100 m, as well as the power data output from the turbine for each method.

Table 2. Statistical comparison between the measured speeds at the height of 100 m and Uequ obtained through the REWS method.

Metrics	100(m/s)	P100(MW)	Uequ(m/s)	PUequ(MW)
Average	6.51	0.96	5.33	0.56
Median	6.40	0.75	5.30	0.42
StD	2.26	0.69	1.63	0.44
Minimum	0.00	0.00	0.00	0.00
Maximum	14.20	2.30	10.50	2.30
Amplitude	14.20	2.30	10.50	2.30
1º Quatile	5.20	0.40	4.40	0.27
3º Quartile	7.90	1.48	6.30	0.71
IQR	2.70	1.08	1.90	0.44

The availability of equivalent wind data is lower compared to the data measured at 100 m because if any of the measurements at any height are missing during a certain period, it renders the calculation unfeasible. To ensure a fair comparison, all periods where equivalent wind data was unavailable were excluded from the analysis, and corresponding data at 100 m were also removed.

This comparison highlights that the equivalent wind speed (Ueq) method tends to produce lower average wind speeds and power outputs compared to the measurements at 100 m. This is due to the Ueq method's consideration of wind speed variations across different heights, providing a more conservative estimate of wind power potential. Consequently, while the 100 m measurements may overestimate the power output, the Ueq method offers a more comprehensive and accurate representation of the wind energy available across the entire rotor swept area.

5. RESULTS

After applying both the traditional method, which uses the wind speed at the turbine hub height, and the equivalent wind speed methodology described by (Wharton and Lundquist, 2012). Figure Fig. (9) presents the results obtained with each of these methods.

As illustrated in Fig. (9), two histograms are presented. We observe two lines: the first, a solid red line, represents the cut-in speed of the turbine, while the second, a dashed red line, indicates the rated speed.

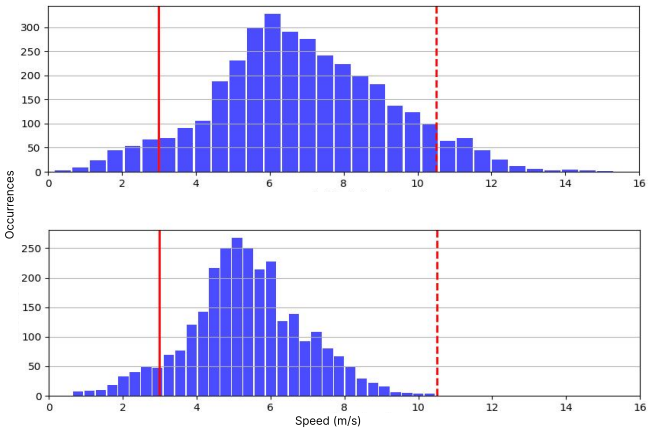

Figure 9. Histogram of turbine-ready wind.

In the first histogram, which represents the hub height method, most data points are between the cut-in speed and the rated speed for this turbine, with peaks reaching approximately 300 occurrences at around 6 m/s. This histogram also indicates that the highest data distribution lies between 6 m/s and 10 m/s.

While the second one represents the equivalent wind speed method. It shows a decrease in the occurrence of higher wind speeds. The peaks reach around 250 occurrences, with wind speeds slightly lower, about 5 m/s. This approach considers the variation in wind speed across the entire turbine rotor, providing a more accurate estimate of the available energy.

With this power data, we can appropriately transform it into daily power normalized by daily availability. The results of this process can be seen in Fig. (10)

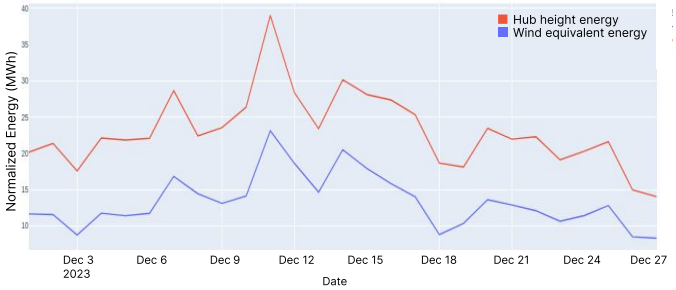

Figure 10. Daily Energy Normalized by Daily Availability.

In Fig. (10), the red line represents the hub height energy, showing a maximum peak of approximately 39 MWh. In contrast, the blue line, representing the equivalent wind speed energy, reaches a peak close to 23 MWh. To complement this analysis, Table 3 presents the capacity factors normalized by data availability calculated for each day using both the traditional hub height method and the REWS method. This table highlights the differences in energy modeling between both approaches.

The significant difference between the two methods is due to the way each methodology accounts for wind speed variations. The hub height method measures wind

speed at a single height, typically resulting in higher wind speed values because it does not account for variations at different heights. This often leads to overestimation of the available energy.

In contrast, the REWS (Rotor Equivalent Wind Speed) method integrates wind speed measurements across the entire rotor swept area. This method considers the vertical wind shear and provides a more conservative and realistic estimate of the wind energy potential. Therefore, while the hub height method shows higher energy peaks, the REWS method offers a more accurate representation of the wind conditions experienced by the turbine, leading to lower but more reliable energy output estimates.

Table 3. Capacity Factor.

Day	Capacity Factor Equivalency	Capacity Factor 100m
1	0.211049	0.365038
2	0.209499	0.387242
3	0.158458	0.318257
4	0.212981	0.400829
5	0.206402	0.395464
6	0.212614	0.400041
7	0.304970	0.519242
8	0.261468	0.405764
9	0.237304	0.426573
10	0.255798	0.477928
11	0.418968	0.706727
12	0.337409	0.513862
13	0.265559	0.423977
14	0.371539	0.546224
15	0.324825	0.509288
16	0.286590	0.495677
17	0.253907	0.458752
18	0.159561	0.337922
19	0.187123	0.328423
20	0.246717	0.425008
21	0.233481	0.397768
22	0.219193	0.403758
23	0.192724	0.346190
24	0.206948	0.367712
25	0.232050	0.391392
26	0.153996	0.271443
27	0.150538	0.254009

The Equivalent Wind Speed (REWS) methodology provides a useful means to understand the effects of wind shear in the context of energy generation. Comparing the equivalent wind speed with measurements taken directly at hub height,Table 3, it was found that the REWS methodology consistently produces lower capacity factor values. For instance, the maximum equivalent capacity factor was 0.418968, while the maximum CF for a 100 m estimation was 0.706727.

To verify which methodology provides a more accurate power assessment, it would be necessary to compare data from the actual power output of a turbine with the modeled power output using wind data measured by a profiler. As we do not have access to this data, we can only conclude that the REWS approach in this location underestimated the energy production, whereas the traditional method at hub height tends to overestimate it. However, the REWS methodology considers more data points that the wind turbine would actually perceive.

The REWS methodology provides a lower but more realistic capacity factor because it takes into account the wind speed variations along the entire rotor swept area, resulting in a more conservative estimate. On the other hand, the hub height method tends to overestimate the capacity factor as it relies on wind speed measurements at a single height, ignoring the variability in wind speed at different heights. This comprehensive approach by the REWS method ensures that all the relevant wind speed data influencing the turbine's performance are considered, thus providing a more accurate and reliable estimation of the wind energy potential.

6. CONCLUSION

During the measurement period, the SODAR faced challenges with energy supply and data losses due to equipment characteristics. A dedicated nanogrid was necessary to mitigate these issues, but data availability still decreased with height, being 94% at 40 m and only 73% at 160 m.

The Equivalent Wind Speed (REWS) methodology was valuable for understanding wind variation effects on energy generation. REWS consistently produced lower average values compared to hub height measurements. For example, the maximum equivalent capacity factor was 0.418968, while the maximum capacity factor at 100 m was 0.706727, indicating that REWS tends to underestimate energy production, whereas the traditional method tends to overestimate it.

REWS offers a more stable and accurate estimate of wind energy generation, with less variability in energy production. However, its effectiveness is limited by data availability at all rotor heights. To confirm the accuracy of REWS, data from the actual power output of a turbine compared to the modeled power output using SODAR measured wind data would be necessary. This highlights the importance of REWS whilst providing a comprehensive and accurate assessment of wind turbine performance, offering insights for optimizing future wind farm projects in the region.

Future approaches could include the integration of long-term wind data, using additional measurement devices, such as LIDAR, to further validate the findings of this preliminary assessment. Additionally, utilization of machine learning algorithms to predict wind patterns and optimize turbine placement could enhance the study's robustness. Investigating the impact of seasonal variations on wind patterns and energy production could also provide valuable insights for future projects.

In summary, this study indicates significant potential for wind energy generation in the Rio Mearim region, i.s Perizes, especially when considering the REWS methodology. This approach provides a more accurate assessment of wind resources, contributing to better management and planning of wind energy installations and promoting a more efficient and sustainable transition to renewable energy sources in the region. This potential was observed even during 2023, an atypical year, with rains occurring at the end of the year instead of the usual pattern at the beginning of the year.

ACKNOWLEDGMENT

This study was financed in part by the Coordenação de Aperfeiçoamento de Pessoal de Nível Superior - Brasil (CAPES) - Finance Code 001, by the Fundação de Amparo à Pesquisa e ao Desenvolvimento Científico e Tecnológico do Maranhão (FAPEMA) (Grant INCT- 05547/17 and Grant BM-05695/23) and by the Conselho Nacional de Desenvolvimento Científico e Tecnológico (CNPq) (Grant 465672/2014-0).

REFERENCES

ABEEÓLICA (2022). Boletim anual: 2022. URL `https://abeeolica.org.br/wp-content/uploads/2023/06/Boletim-de-Geracao-Eolica-2022.pdf`. Access date: 04/01/2024.

Cosme, D.L., Veras, R.B., Camacho, R.G., Saavedra, O.R., Torres, A., and Andrade, M.M. (2023). Modeling and assessing the potential of the boqueirão channel for tidal exploration. *Renewable Energy*, 219, 119468.

Costa, A.M.S., de Araujo Soares, R., de Sousa Veras, R.B., Torres, A.R., Cosme, D.L.S., and Saavedra, O.R. (2023). Preliminary assessment of the potential for tidal currents in the boqueirão channel. In *Renewable Resources and Energy Management*, 99–106. CRC Press.

Dantas, E.J.d.A., Rosa, L.P., da Silva, N.F., and Pereira, M.G. (2019). Wind power on the brazilian northeast coast, from the whiff of hope to turbulent convergence: The case of the galinhos wind farms. *Sustainability*, 11(14), 4–6. doi:10.3390/su11143802.

Figueredo, W.M., Veras, R.B.d.S., Costa, A.M.S., Soares, R.d.A., Saavedra, O.R., and Leite Neto, P.B. (2023). "Avaliação Preliminar de Energia Éolica e de Correntes de Maré na Região da Ilha do Caranguejo - Foz do Rio Mearim". Simpósio Brasileiro de Sistemas Elétricos - SBSE.

Martins, A.V.C., Oliveira, D.Q., Pimenta, F., and Veras, R.B. (2023). Influence of vertical wind shear on the annual energy production of a coastal region in north-eastern brazil. In *2023 Workshop on Communication Networks and Power Systems (WCNPS)*, 1–7. IEEE.

ONS (2023). Fator de capacidade. URL `https://www.ons.org.br/Paginas/resultados-da-operacao/historico-da-operacao/fator-capacidade.aspx`. Access date: 04/01/2024.

Panofsky, H.A. and Townsend, A. (1964). Change of terrain roughness and the wind profile. *Quarterly Journal of the Royal Meteorological Society*, 90(384), 147–155.

Sumner, J. and Masson, C. (2006). Influence of atmospheric stability on wind turbine power performance curves.

The-Wind-Power (2018). Siemens swt-2.3-113. URL `https://www.thewindpower.net/turbine_en_749_siemens_swt-2.3-113.php`. Update for this sheet: 4 June 2018. Complete/correct this sheet.

Wharton, S. and Lundquist, J.K. (2012). Atmospheric stability affects wind turbine power collection. *Environmental Research Letters*, 7(1), 014005.